Monthly Notices of the ROYAL ASTRONOMICAL SOCIETY

MNRAS **532,** L21–L26 (2024) https://doi.org/10.1093/mnrasl/slae038
Advance Access publication 2024 May 6

Optical spectroscopic and photometric classification of the X-ray transient EP240309a (EP J115415.8−501810) as an intermediate polar

Stephen B. Potter ,[1,2★] David A. H. Buckley ,[1,3,4] S. Scaringi ,[5] I. M. Monageng ,[1,3] Okwudili D. Egbo,[1,3] Philip A. Charles,[4,6] N. Erasmus,[1] Carel van Gend,[1] Egan Loubser,[1] Keegan Titus,[1] Kathryn Rosie,[1] Hitesh Gajjar,[1] H. L. Worters,[1] Sunil Chandra ,[1,7] R. P. M. Julie[8] and Moloko Hlakola[1]

[1]*South African Astronomical Observatory, PO Box 9, Observatory 7935, Cape Town, South Africa*
[2]*Department of Physics, University of Johannesburg, PO Box 524, Auckland Park 2006, South Africa*
[3]*Department of Astronomy, University of Cape Town, Private Bag X3, Rondebosch 7701, South Africa*
[4]*Department of Physics, University of the Free State, PO Box 339, Bloemfontein 9300, South Africa*
[5]*Centre for Extragalactic Astronomy, Department of Physics, Durham University, South Road, Durham, DH1 3LE, UK*
[6]*Department of Physics and Astronomy, University of Southampton, Southampton, SO17 1BJ, UK*
[7]*Center for Space Research, North-West University, Potchefstroom 2520, South Africa*
[8]*South African Radio Astronomy Observatory, 2 Fir Street, Observatory 7925, Cape Town, South Africa*

Accepted 2024 April 29. Received 2024 April 25; in original form 2024 April 19

ABSTRACT

We report on optical follow-up observations of an X-ray source initially detected by the Einstein Probe mission. Our investigations categorize the source as an intermediate polar, a class of magnetic cataclysmic variables, exhibiting an orbital period of 3.7614(4) h and a white dwarf spin period of 3.97 min. The orbital period was identified through *TESS* observations, while our high-speed photometric data, obtained using the 1.9m and Lesedi 1.0m telescopes at the South African Astronomical Observatory, revealed both the spin and beat periods. Additionally, we present orbitally phase-resolved spectroscopic observations using the 1.9m telescope, specifically centred on the H β emission line, which reveal two emission components that exhibit Doppler variations throughout the orbital cycle.

Key words: accretion, accretion discs – stars: individual: EP J115415.8−501810 – novae, cataclysmic variables.

1 INTRODUCTION

Ling et al. (2024) reported the detection of a new, highly variable X-ray source, designated EP240309a/EP J115415.8−501810, by the Einstein Probe (EP) mission (Yuan et al. 2022), using the Wide-field X-ray Telescope on board, during a calibration observation on 2024 March 9. The source exhibited significant variability, with its 0.5–4 keV flux ranging between 5×10^{-12} to 7×10^{-12} erg cm^{-2} s^{-1}, until 2024 March 16. It was subsequently detected by the Follow-up X-ray Telescope (FXT) on board EP, on March 2024 16. Historical observations were examined, revealing a potential identification with XMMSL J115415.6−501758, a source previously detected by *XMM–Newton* and *Swift*/XRT, albeit with variable flux levels across observations. Consistent with the FXT observations, *eROSITA* detected a faint source, 1eRASS J115415.7−501758, in its first six months of the all-sky survey (Merloni et al. 2024). Ling et al. (2024) also noted a highly variable, bright UV counterpart (*Gaia* DR3 5370642890382757888) suggesting that it is likely of Galactic origin and potentially a candidate Cataclysmic Variable (CV) thereby encouraging follow-up observations.

On 2024 March 30, Chang et al. (2024) conducted follow-up radio observations at 1.28 GHz, but no radio counterpart was found within the error circle of the EP X-ray position, nor at the position of the bright UV source.

Rodriguez & Kulkarni (2024) analysed the *Gaia* XP spectrum and the ASAS-SN light curve, reporting erratic variability in the observed data. Based on these observations, they suggested that the object (hereafter referred to as EP240309a) in question is a magnetic CV.

Buckley et al. (2024) conducted observations of EP240309a using the Southern African Large Telescope (SALT; Buckley, Swart & Meiring 2006) on 2024 March 19. Their findings revealed a spectrum characterized by broad emission lines, echoing the observations made with the lower resolution spectrum from *Gaia* (Rodriguez & Kulkarni 2024). The spectrum displays a steeply rising blue continuum, prominently featuring strong Balmer and He I lines, alongside He II 4686 and the Bowen fluorescence C III/N III blend (4640–4650 A). Buckley et al. 2024 also reported the detection of a 3.762 h period in the *TESS* light curve, consistent with an orbital period.

2 OBSERVATIONS

V and *g* filtered observations were obtained from the ASAS-SN Sky Patrol Photometry Data base, see Hart et al. (2023) and Shappee et al. (2014). The observations cover a time span of ∼8.3 yr with a cadence of ∼1 measurement every few days (Fig. 1).

★ E-mail: sbp@saao.ac.za

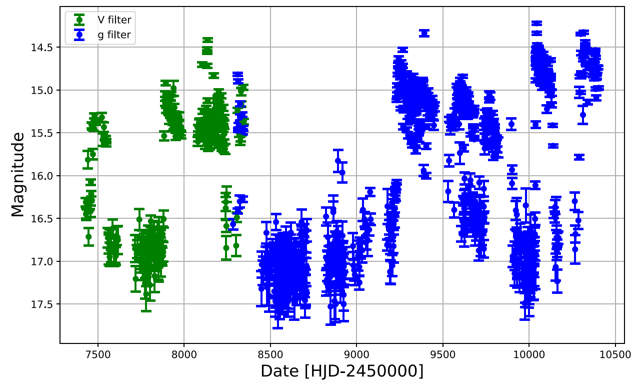

Figure 1. *V* and *g* filtered light curves from ASAS-SN.

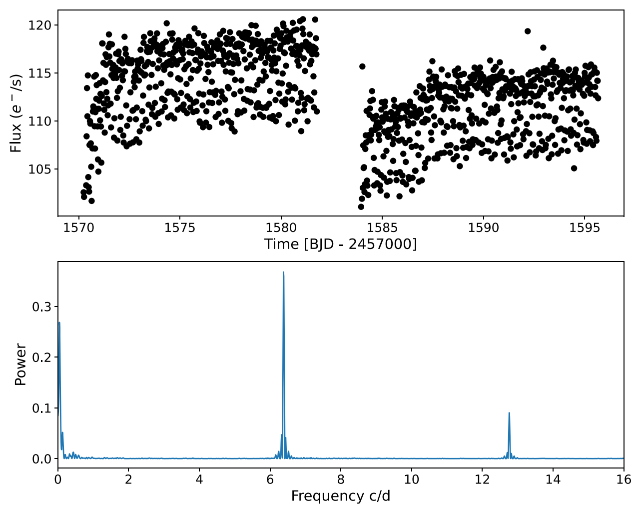

Figure 2. *Upper plot*: the *TESS* light curve of EP240309a spanning ∼25 d. *Lower plot*: the corresponding Lomb–Scargle Periodogram of the mean subtracted curve.

Optical photometric observations of EP240309a were obtained using the *Transiting Exoplanet Survey Satellite* (*TESS*) that cover 25 d (2019 Mar 26–2019 Apr 22) with a cadence of ∼50 data points per day (Fig. 2). There also exists an available ELEANOR light curve (Feinstein et al. 2019) which was downloaded from the Mikulski Archive for Space Telescopes (MAST).

Following the transient alert (Ling et al. 2024) observations were promptly secured through the SAAO Intelligent Observatory programme (Potter et al. 2024). We obtained high cadence (10 s) i' and R filtered photometric observations with the 1.9-m and 1.0-m Lesedi telescopes of the South African Astronomical Observatory using the SHOCNWONDER and Mookodi instruments (see Table 1) in 2024 March and April. Differential photometry was derived (Fig. 3) using the Tea-PHOT data reduction package (Bowman & Holdsworth 2019).

As originally reported in Buckley et al. (2024), SALT spectroscopy was obtained using the Robert Stobie Spectrograph (RSS; Burgh et al. 2003; Kobulnicky et al. 2003) in long-slit low-resolution mode ($R \sim 800$), with an exposure time of 1200 s, covering a wavelength range of 3500–7500 Å (see Table 1). Data reduction was carried out using the PYSALT[1] software package (Crawford et al. 2010). The spectrum is displayed in Fig. 4 where the two gaps are due to the detector consisting of a mosaic of three chips which in turn results in two small gaps in the wavelength dispersion direction. Relative flux calibration was achieved using sensitivity functions derived from observations of the spectrophotometric standard star HILT 600 (HD 289002).

Spectroscopic observations were obtained using the SPUPNIC instrument (Crause et al. 2019) of the SAAO 1.9m telescope. A total of ∼15.8 h spread over 4 nights with a 500 s exposure time. Grating 4 was used with a dispersion of 1.3 Å pixel^{-1} covering a wavelength range of 4200–5000 Å, utilizing a slit width of 1.5arc-seconds and centred on the Hβ emission line (see Table 1). Comparison arc (Cu–Ar) spectra were taken at regular intervals for wavelength calibration, however the data have not been flat-fielded or flux calibrated. Data reductions proceeded using standard IRAF[2] routines.

3 RESULTS

3.1 Photometry: ASAS-SN

Fig. 1 shows the archival V and g filtered observations from the ASAS-SN survey spanning ∼8.3 yr. Originally reported in Rodriguez & Kulkarni (2024) as showing erratic variability between $V = 17.2$ and 14.4 mag, upon closer examination the light curve appears to have a bimodal distribution of variability. This can typically be understood as characteristic behaviour of magnetic CVs during transitions in accretion states, although it is more frequently observed in the synchronized polar subclass and is also prevalent in nova-like variables. The origin of high and low-luminosity/accretion states is not yet fully understood and it has been suggested that such changes are due to star-spots and solar-type magnetic cycles in the donor star (e.g. Livio & Pringle 1994; Kafka & Honeycutt 2005)

3.2 Photometry: *TESS*

Despite the low cadence, the 'banding' visible in the light curve Fig. 2 is indicative of a periodic signal. This is confirmed with a Lomb–Scargle Periodogram, Fig. 2, showing a dominant frequency at 6.3806(6) c/d [3.7614(4) h] and its harmonic. Errors in the recovered period were determined via bootstrapping the *TESS* light curve with replacement. We identify this as the orbital period of EP240309a, in agreement with the original report in Buckley et al. (2024).

3.3 Photometry: Lesedi & 1.9m

Both i' and R light curves (e.g. Fig. 3) exhibit variability on the scale of hours, as well as more frequent fluctuations, consistent with flickering as seen in most CVs (Scaringi 2014). To analyse these variations, we conducted a Lomb–Scargle Periodogram analysis on the aggregated light curves (see Fig. 5).

At the lower frequency end, we detected peaks corresponding to the orbital period and its second and third harmonics. Additionally, the periodogram revealed a frequency of 362.5 c/d (equivalent to 3.972 min), which we associate with the spin period of the white dwarf, as denoted by the blue dashed line in Fig. 5 and its top inset.

[1]For more details on pysalt visit http://pysalt.salt.ac.za/.
[2]IRAF is distributed by the National Optical Astronomy Observatories, which are operated by the Association of Universities for Research in Astronomy, Inc., under cooperative agreement with the NSF.

Table 1. Log of observations.

Date	BJD − 2400000.0(TDB) start	Telescope	Instrument	Filter/ Grating Res.	Exposure	Total time h
2024-03-19	60388.55226(JD)	SALT	RSS	$R \sim 800$	1200 s	1200 s
2024-03-24	60394.29718435	1.9m SAAO	SPUPNIC	1.3 Å/pix	21 × 500 s	3.25
2024-03-26	60396.2379825	Lesedi (1.0m) SAAO	Mookodi	*i’*	10 s	2.45
2024-03-28	60398.28792416	1.9m SAAO	SPUPNIC	1.3 Å/pix	26 × 500 s	3.62
2024-03-29	60399.30361589	1.9m SAAO	SPUPNIC	1.3 Å/pix	20 × 500 s	2.71
2024-04-01	60402.26767327	1.9m SAAO	SPUPNIC	1.3 Å/pix	45 × 500 s	6.30
2024-04-02	60403.33377779	1.9m SAAO	SHOCNWONDER	*R*	10 s	6.74

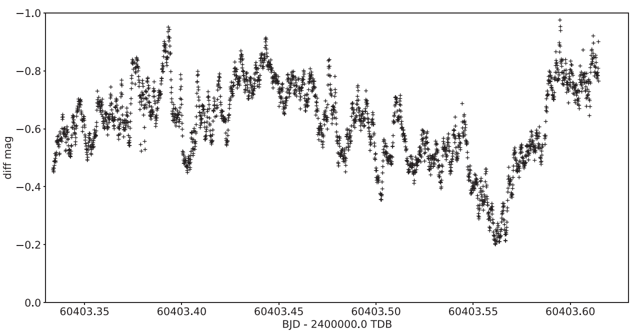

Figure 3. Example photometry, showing *R* filtered photometric observations made with the SHOCNWONDER instrument on the SAAO 1.9m telescope spanning 6.74 h on 2024 2 April.

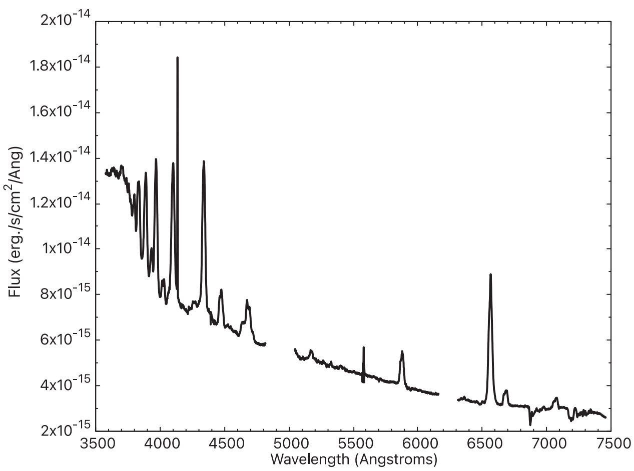

Figure 4. Optical spectrum of EP240309a from SALT.

The top inset of Fig. 5 also features a green dashed line indicating the beat frequency ($\omega - \Omega$) which coincides with a prominent peak in the periodogram. Moreover, the periodogram depicted in the lower right inset reveals the presence of (2ω) and ($2\omega - 2\Omega$) frequencies.

We also observe a notable frequency around 60.5 c/d, roughly in-between 9Ω and 10Ω, which does not correspond to any harmonics of the identified frequencies. Further observations are necessary to determine whether this represents a transient signal.

In summary, we have identified the orbital and spin frequencies as 6.3806(6) c/d and 362.5(1) c/d, respectively, based on data from *TESS* (for the orbit) and combined observations from Lesedi and the 1.9m telescopes (for the spin). The uncertainties in the spin frequency, indicated in parentheses, was measured from the full width at half maximum (FWHM) of the periodogram peak, taking into account potential aliases.

In Fig. 6, we present the spin and beat-folded light curves derived from the more extensive 1.9m photometric observations, illustrated in the lower left and right panels, respectively. Both types of light curves reveal the presence of single pulses. The upper panels of Fig. 6 depict the evolution of consecutive spin and beat-folded light curves throughout the orbital cycle. It is important to note that each successive folded light curve has undergone normalization to mitigate the dominant higher amplitude orbital modulation. Within the constraints of the signal-to-noise ratio of our observations, we observe that the spin pulse remains relatively stable in phase throughout the orbital cycle. In contrast, the beat pulse evolves to progressively earlier beat phases as the orbital cycle progresses. This observation suggests that the emission source responsible for the high-frequency pulses is anchored in the frame of the rotating white dwarf, rather than resulting from reprocessed emission originating from a location locked in the orbital frame. The latter scenario would result in a beat pulse that remains constant over the orbital cycle.

A detailed examination of orbital phases ∼0.1–0.2, as shown in the top panels of Fig. 6, uncovers what seems to be a swift advancement of both the spin and beat pulses by a complete cycle. This observation may suggest that, for the majority of the time, a single spin-dominating pulse is present, likely originating near an accreting magnetic pole of the white dwarf. However, it appears that, on occasion, accretion may transition to the opposite magnetic pole, causing a pulse that exhibits a shift by ∼half a spin/beat cycle and then another ∼half a spin/beat cycle when reverting back to the original pulse.

3.4 *Gaia*: astrometry and spectrum

As reported in Rodriguez & Kulkarni (2024), EP240309 is a *Gaia* (Gaia Collaboration 2016) source in the Data Release 3 catalogue (DR3 5370642890382757888; Gaia Collaboration 2023), at a magnitude of $G = 16.2$. Astrometry for the source gives a parallax of 3.2041 mas and proper motion of 68.270 mas yr^{-1}. The distance determined from Bailer-Jones et al. (2021) is $d = 309.5 \pm 0.4$ pc.

Furthermore, *Gaia* produced a low resolution ($R = 30$–100) XP continuous spectrum, which is shown in Fig, 7. The spectrum is typical of a CV, suggested by Rodriguez & Kulkarni (2024; notwithstanding the low spectral resolution) to possibly be a magnetic CV, based on the presence of He II 4686 Å, a high excitation line which is prominent in these relatively X-ray luminous CV systems.

3.5 Spectroscopy: SALT

Pronounced broad emission lines are seen, similar to what is reported for the lower resolution *Gaia* spectrum (Rodriguez & Kulkarni 2024),

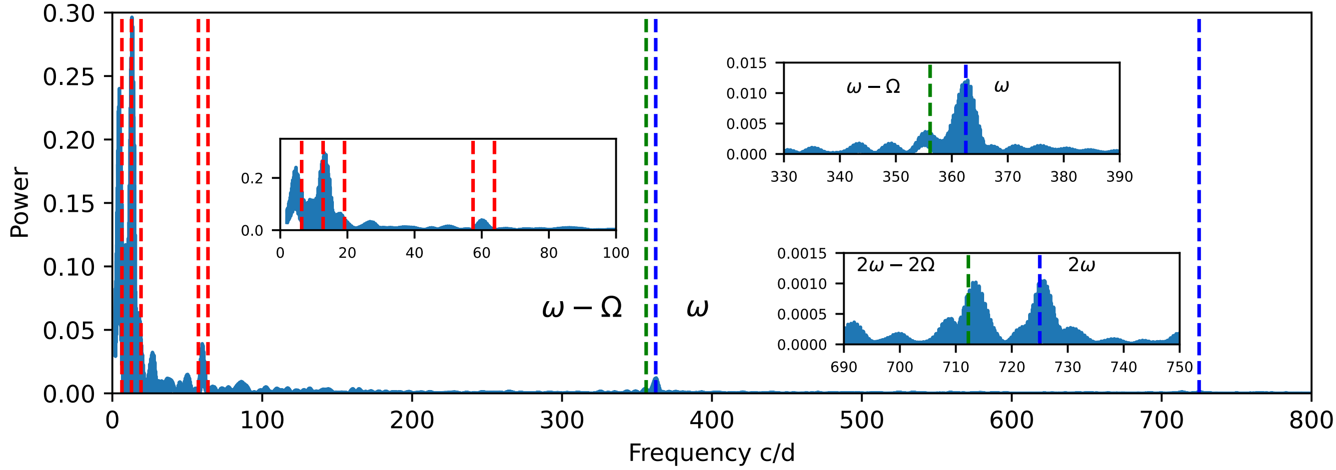

Figure 5. Lomb–Scargle Periodogram of the combined 3.25 h and 6.74 h i', R filtered photometry. Periodgrams of individual light curves show similar results (not shown). Assumed $\Omega = 6.3796 = 3.762$ h. Left inset: red dashed lines correspond to Ω, 2Ω, 3Ω, 9Ω, 10Ω. Top inset: blue dashed line indicates possible $\omega = 362.5 = 3.97$ mins and green indicates $\omega - \Omega$. Note the peak between frequencies 9Ω and 10Ω also present on individual nights (not shown).

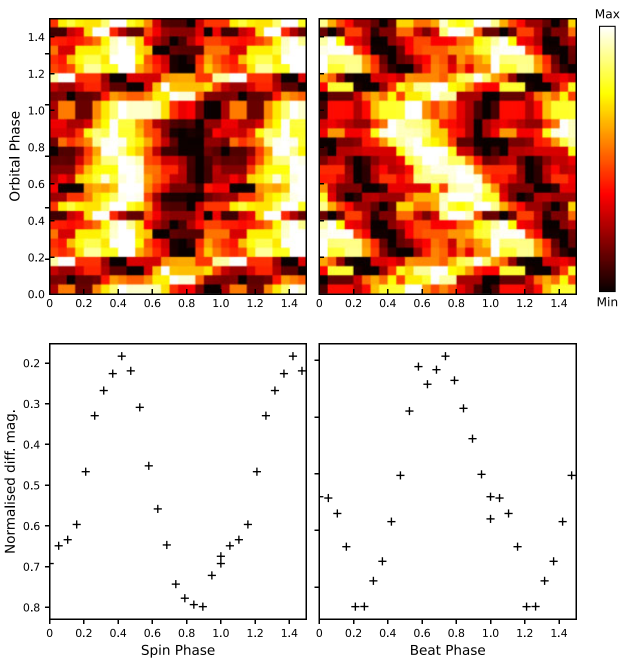

Figure 6. *Top left*: evolution of the spin pulse over the orbital period. *Top right*: evolution of the beat pulse over the orbital period. Bottom left: 1D normalized spin-folded and binned light curve. Bottom right: 1D normalized beat-folded and binned light curve.

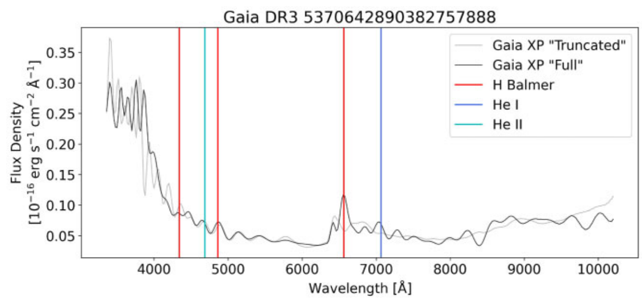

Figure 7. *Gaia* XP continuous spectrum of EP240309a, showing strong emission lines on a blue continuum, typical of a CV.

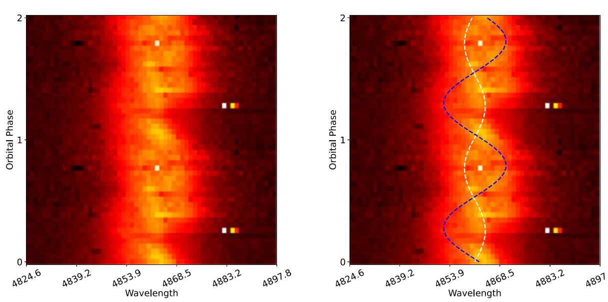

Figure 8. Left plot shows all the spupnic observations of EP240309a centred on H β folded and binned on the assumed orbital period of 3.764 h. Right plot: same as left but overlaid with two sine functions indicating two possible components.

on a steeply rising blue continuum (see Fig, 4). In addition to strong Balmer and He I lines (4471, 5018, 5876, 6678, 7065 Å), the He II 4686 and Bowen fluorescence C III/N III blend (4640–4650 Å) are also prominent. Due to the chip gap in the RSS detector, the H β line was missed. H α is characterized by a FWHM of around 1500 km s^{-1}.

3.6 Spectroscopy: SAAO, 1.9m

The left panel of Fig. 8 displays the phase-folded spectroscopic observations from the SAAO 1.9m telescope, centred on the H β emission line. Despite the low signal-to-noise ratio in individual spectra, it is evident from this figure that H β is composed of multiple components exhibiting Doppler variations throughout the orbital cycle. Upon careful examination, we tentatively discern two distinct components, which are highlighted by dashed curves in the right panel of Fig. 8 to guide the eye. Although the H β Doppler tomogram, which is not depicted here, reveals two areas of intensified emission, the absence of an accurately determined orbital ephemeris precludes the correct phasing and therefore the identification of these features in relation to the binary system's components. The FWHM of H β is approximately 1500 km s^{-1}, corroborating findings from an earlier SALT observation.

4 SUMMARY AND DISCUSSION

Prompted by the detection of a transient X-ray source, EP240309a, through the EP mission, we embarked on an optical follow-up campaign. A Lomb–Scargle period analysis of *TESS* observations disclosed a predominant period of 3.7614(4) h, indicating the likely binary orbital period. This was corroborated by our high-speed photometric observations at SAAO, which additionally unveiled frequencies consistent with a white dwarf spin period of 3.97 min and the corresponding beat frequency. These findings categorize the source as an intermediate polar.

Our analysis of the long-term light curve from the ASAS-SN archive indicated almost bimodal transitions between brightness levels, a behaviour typically observed during the high and low state transitions in magnetic CVs (see e.g. Kafka & Honeycutt 2005) further corroborating our IP classification.

Spectroscopic examination using SALT revealed the characteristic broad emission line spectrum typical of magnetic CVs. Moreover, time-resolved SAAO (1.9m) spectroscopic observations centred on the H β emission identified two Doppler variations across the orbital cycle. The typical double-peaked lines emission expected in a disc accreting system (see e.g. Mhlahlo et al. 2007) was not seen although this would be best confirmed with better signal-to-noise observations. To accurately phase our observations and determine the origin of these Doppler varying components, further time-resolved spectroscopic observations, for instance of the Ca II triplet from the irradiated face of the secondary star, are required (see e.g. Khangale et al. 2020).

We encourage further more detailed follow-up X-ray observations in order to ascertain the X-ray spectral properties and also the spin and/or beat temporal behaviour. This will help to reveal the accretion dynamics e.g. disc-fed or disc-stream overflow and also whether the system is a hard or soft X-ray source (e.g. Joshi et al. 2023; Vermette et al. 2023). Similarly time-resolved photopolarimetry will further enhance our understanding of the accretion dynamics and the overall energetics (e.g. Potter et al. 2012).

In Fig. 9, we show the position of EP23409a in the $P_{\rm spin}$–$P_{\rm orb}$ diagram (Norton et al. 2008), together with other IPs and related objects. The four fastest spinning systems are represented by the bottom two red circles and crosses, with CTCV J2056−3014 and V1460 Her, the left and right circles, respectively. The propeller systems, LAMOST J024048+195226 and AE Aqr, are the left and right red crosses, respectively.

It is interesting to note that the orbital period and the fast spin period of EP240309a fall mid-way between those of the two known so called white dwarf pulsar systems (small red stars in Fig. 9), AR Sco (Marsh et al. 2016) and J191213.72−441045 (Pelisoli et al. 2023; Schwope et al. 2023). These two exceptional systems are characterized with properties that set them aside from all other known CV systems, namely strong pulsed emission on the white dwarf spin period, detectable from radio to X-rays including optical polarization (Buckley et al. 2017; Potter & Buckley 2018; Pelisoli et al. 2023) with no signs of accretion. We do not yet fully understand either what evolutionary path AR Sco and J191213.72−441045 followed, or what underlying physical characteristics of the binary constituents set them so apart from other CVs and in particular intermediate polars. Given its similarities to these systems in terms of basic stellar constituents, periods, and binary size, EP240309a clearly warrants further detailed investigation.

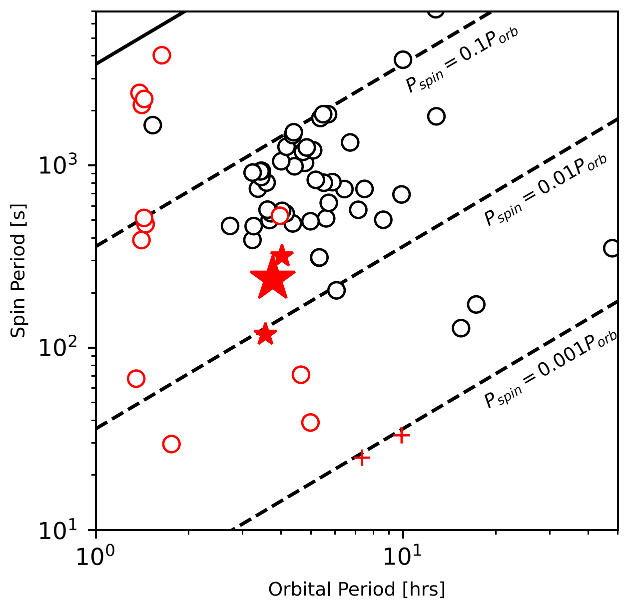

Figure 9. Orbital versus spin period of the so-called ironclad intermediate polars, based on data compiled by Koji Mukai (https://asd.gsfc.nasa.gov/Koji.Mukai/iphome/iphome.html) The large red star represents EP240309a, small red stars denote the two known white dwarf pulsar systems, red crosses denote the two propeller systems (AE Aqr and LAMOST J024048.51+195226.9) and open red circles illustrate low-luminosity IPs (Pretorius & Mukai 2014).

ACKNOWLEDGEMENTS

The spectroscopic observations with the Southern African Large Telescope (SALT) were obtained under the programme 2021-2-LSP-001 (PI: David Buckley). Other ground-based observations were obtained with the facilities of the SAAO Sutherland observing station.

This paper includes data collected by the *TESS* mission, which are publicly available from the Mikulski Archive for Space Telescopes (MAST). Funding for the *TESS* mission is provided by NASA's Science Mission directorate.

The *Gaia* XP Continuous spectrum was obtained from the *Gaia* DR3. This work has made use of data from the European Space Agency (ESA) mission *Gaia* (https://www.cosmos.esa.int/gaia), processed by the *Gaia* Data Processing and Analysis Consortium (DPAC, https://www.cosmos.esa.int/web/gaia/dpac/consortium). Funding for the DPAC has been provided by national institutions, in particular the institutions participating in the *Gaia* Multilateral Agreement.

DAHB would like to thank Tony Rodriguez for useful discussions. DAHB and SBP acknowledge research support from the National Research Foundation. SS was supported by STFC grant ST/X001075/1. IMM was supported by the South African NRF and the UCT VC 2030 Future Leaders Programme. PAC acknowledges the Leverhulme Trust for an Emeritus Fellowship.

We thank the referee for a very quick and positive response and suggesting Fig. 9.

DATA AVAILABILITY

The reduced data underlying this article will be shared on reasonable request to the corresponding author.

REFERENCES

Bailer-Jones C. A. L., Rybizki J., Fouesneau M., Demleitner M., Andrae R., 2021, AJ, 161, 147
Bowman D. M., Holdsworth D. L., 2019, A&A, 629, A21
Buckley D. A. H., Meintjes P. J., Potter S. B., Marsh T. R., Gänsicke B. T., 2017, Nat. Astron., 1, 0029
Buckley D. A. H., Monageng I., Aydi E., Scaringi S., Charles P. A., 2024, Astron. Telegram, 16554, 1
Buckley D. A. H., Swart G. P., Meiring J. G., 2006, Proc. SPIE Conf. Ser. Vol. 6267, Ground-based and Airborne Telescopes. SPIE, Bellingham, p. 62670Z
Burgh E. B., Nordsieck K. H., Kobulnicky H. A., Williams T. B., O'Donoghue D., Smith M. P., Percival J. W., 2003, in Iye M., Moorwood A. F. M., eds, Proc. SPIE Conf. Ser. Vol. 4841, Instrument Design and Performance for Optical/Infrared Ground-based Telescopes. SPIE, Bellingham, p. 1463
Chang N. et al., 2024, Astron. Telegram, 16572, 1
Crause L. A. et al., 2019, J. Astron. Telesc. Instrum. Syst., 5, 024007
Crawford S. M. et al., 2010, Proc. SPIE Conf. Ser. Vol. 7737, Observatory Operations: Strategies, Processes, and Systems III. SPIE, Bellingham, p. 773725
Feinstein A. D. et al., 2019, PASP, 131, 094502
Gaia Collaboration, 2016, A&A, 595, A1
Gaia Collaboration, 2023, A&A, 674, A1
Hart K. et al., 2023, preprint (arXiv:2304.03791)
Joshi A., Rawat N., Schwope A., Pandey J. C., Scaringi S., Sahu D. K., Rao S. M., Singh M., 2023, MNRAS, 521, 6156
Kafka S., Honeycutt R. K., 2005, AJ, 130, 742
Khangale Z. N. et al., 2020, MNRAS, 492, 4298
Kobulnicky H. A., Nordsieck K. H., Burgh E. B., Smith M. P., Percival J. W., Williams T. B., O'Donoghue D., 2003, in Iye M., Moorwood A. F. M., eds, Proc. SPIE Conf. Ser. Vol. 4841, Instrument Design and Performance for Optical/Infrared Ground-based Telescopes, SPIE, Bellingham, p. 1634
Ling Z. X. et al., 2024, The Astron. Telegram, 16546, 1
Livio M., Pringle J. E., 1994, ApJ, 427, 956
Marsh T. R. et al., 2016, Nature, 537, 374
Merloni (2024) Astronomy & Astrophysics, A34 , 0004-6361
Mhlahlo N., Buckley D. A. H., Dhillon V. S., Potter S. B., Warner B., Woudt P. A., 2007, MNRAS, 378, 211
Norton A. J., Butters O. W., Parker T. L., Wynn G. A., 2008, ApJ, 672, 524
Pelisoli I. et al., 2023, Nat. Astron., 7, 931
Potter S. B., Buckley D. A. H., 2018, MNRAS, 481, 2384
Potter S. B., Romero-Colmenero E., Kotze M., Zietsman E., Butters O. W., Pekeur N., Buckley D. A. H., 2012, MNRAS, 420, 2596
Potter S., Chandra S., Erasmus N., Hlakola M., Julie R., Worters H., van Gend C., 2024, Proc. 19th Int. Conf. Accel. Large Exp. Phys. Control Syst. (ICALEPCS'23). No. 19 in International Conference on Accelerator and Large Experimental Physics Control Systems. JACoW Publishing, Geneva, Switzerland, p. 1
Pretorius M. L., Mukai K., 2014, MNRAS, 442, 2580
Rodriguez A., Kulkarni S. R., 2024, Astron. Telegram, 16549, 1
Scaringi S., 2014, MNRAS, 438, 1233
Schwope A., Marsh T. R., Standke A., Pelisoli I., Potter S., Buckley D., Munday J., Dhillon V., 2023, A&A, 674, L9
Shappee B. et al., 2014, American Astronomical Society Meeting Abstracts #223. p. 236.03
Vermette B. et al., 2023, ApJ, 954, 138
Yuan W., Zhang C., Chen Y., Ling Z., 2022, in Bambi C., Santangelo A., eds, Handbook of X-ray and Gamma-ray Astrophysics. Springer, Singapore, p. 86

This paper has been typeset from a TEX/LATEX file prepared by the author.